



Cite this: *Mater. Chem. Front.*, 2023, 7, 6141

## Recent advances in regulating the excited states of conjugated thermally activated delayed fluorescence polymers for high-efficiency OLEDs

Maoqiu Li,<sup>a</sup> Lei Hua,<sup>a</sup> Junteng Liu<sup>\*b</sup> and Zhongjie Ren<sup>ID \*a</sup>

A detailed overview of thermally activated delayed fluorescence conjugated polymers reported from 2015 to present is provided, with a focus on their molecular structures, excited-state properties, and organic light-emitting diode performance. In addition, the rules for regulating the excited-state properties of these TADF conjugated polymers are summarized. By carefully designing the molecular structures of conjugated TADF polymers, their excited-state properties and the energy gaps between the lowest singlet excited states and the lowest triplet excited state can effectively be adjusted. Furthermore, the reverse intersystem crossing rate of conjugated polymers can be increased by enhancing the spin-orbit coupling effect between the triplet and singlet states, and thus optimizing the collection of triplet excitons and improving the device performance, including external quantum efficiency and efficiency roll-off.

Received 17th July 2023,

Accepted 19th August 2023

DOI: 10.1039/d3qm00799e

rsc.li/frontiers-materials

### 1. Introduction

Organic light-emitting diodes (OLEDs) are widely used in the display (such as smartphones and TV screens) and lighting industries. Over the past 30 years, research and development of OLEDs have rapidly progressed in both academia and industry.<sup>1–4</sup> Phosphorescent materials are now an integral part of OLEDs for mobile displays, which are considered a second-generation OLED material with 100% internal quantum efficiency (IQE).<sup>5</sup> In order to solve the high energy consumption in vacuum evaporation and high-cost dependence of noble metals, Adachi *et al.* proposed a pure organic non-precious metal thermally activated delayed fluorescence (TADF) material, which is considered to be a third-generation OLED emitting material.<sup>6</sup> Through delicate molecular design, the donor and acceptor units in the molecule are distorted, so that the highest occupied orbital (HOMO) and the lowest unoccupied orbital (LUMO) of the molecule are separated to obtain extremely small singlet and triplet energy gaps ( $\Delta E_{ST}$ ).<sup>7</sup> This unexpectedly enables triplet excitons to have the ability to upconvert to singlet states in the absence of heavy metal atoms, so like phosphorescent materials, TADF materials also have 100% exciton utilization.<sup>8</sup> Among them, polymers with natural solution-processable characteristics and good chemical modification are important components of

TADF materials. Inheriting the characteristics of 100% IQE of TADF materials, polymer light-emitting diodes (PLEDs) can be used to easily prepare large-area and high-efficiency light-emitting devices.<sup>4</sup> Generally, according to whether the polymeric main chains are continuously conjugated, polymers can be divided into two categories: non-conjugated and conjugated main chain polymers. PLEDs based on these two series of polymers have achieved rapid development in recent years.<sup>9–12</sup> Furthermore, due to the unique assistance of the conjugated polymer backbone for carrier transport, PLEDs maintain the highest external quantum efficiency (EQE) record of up to 25.4%.<sup>9,13</sup>

The EQE of PLEDs refers to the ratio of the number of photons emitted per unit time to the injected electron–hole pairs and is related to the efficiency of converting electricity into light.<sup>14</sup> It is one of the main performance indicators used to measure PLED devices because it directly determines the brightness and energy efficiency of PLEDs. Recently, in the field of full-colour light, the efficiency of PLEDs has achieved remarkable progress comparable to that of small molecule OLEDs and phosphorescent OLEDs.<sup>15</sup> The 25.4% EQE mentioned above pertains to yellow-emitting PLEDs, and the EQEs of orange-red and blue-green emitting PLEDs have also reached 24.8%<sup>13</sup> and 24%.<sup>16</sup> In addition to pursuing high efficiency, the efficiency roll-off of PLED devices is also one of the performance indicators that researchers pay special attention to. Most PLEDs experience rapid efficiency roll-off at high brightness, which affects device performance and severely hinders commercial applications. The efficiency roll-off of PLEDs originates from the accumulation of emitter triplet excitons.<sup>17</sup>

<sup>a</sup> State Key Laboratory of Chemical Resource Engineering Beijing University of Chemical Technology, Beijing 100029, China. E-mail: renzj@mail.buct.edu.cn

<sup>b</sup> Beijing Key Laboratory of Membrane Science and Technology, Beijing University of Chemical Technology, Beijing 100029, China. E-mail: liut@mail.buct.edu.cn

For TADF materials, increasing the reverse intersystem crossing rate ( $k_{\text{RISC}}$ ) and reducing the triplet exciton quenching are effective ways to reduce the efficiency roll-off.<sup>18</sup>

The typical molecular structure of conjugated TADF polymers usually consists of donor–acceptor,<sup>19</sup> or donor–acceptor–donor,<sup>20</sup> which promotes the formation of intramolecular charge transfer (ICT) states between the donor and acceptor, so is the conjugated TADF polymer. Correspondingly, the lowest singlet excited state ( $S_1$ ) of the molecule is often the charge transfer state ( $^1\text{CT}$ ). For the triplet excited state, it usually displays the charge transfer triplet state ( $^3\text{CT}$ ) and localized excited triplet state ( $^3\text{LE}$ ). In order to improve the EQE of PLEDs and reduce the efficiency roll-off, there are many in-depth studies on the regulation of molecular excited states related to luminescence.<sup>15</sup>

According to Fermi's golden rule, larger  $k_{\text{RISC}}$  requires higher spin orbit coupling (SOC) matrix element values and smaller  $\Delta E_{\text{ST}}$ .<sup>21</sup>

$$k_{\text{RISC}} \propto \frac{\langle S | H_{\text{SOC}} | T \rangle}{\Delta E_{\text{ST}}} \quad (1)$$

where  $k_{\text{RISC}}$  is the rate of RISC,  $\langle S | H_{\text{SOC}} | T \rangle$  is the singlet and triplet SOC constant, and  $\Delta E_{\text{ST}}$  is the singlet and triplet energy gap.

As shown in Fig. 1, based on Fermi's golden rule, two approaches to improving the  $k_{\text{RISC}}$  of conjugated polymers can be easily made: one is to obtain a suitable  $\Delta E_{\text{ST}}$ ; the other is to enhance the spin coupling between singlet and triplet states. From the perspective of enhancing SOC, it can be divided into the  $^3\text{LE}$  auxiliary strategy and the hyperfine coupling (HFC) strategy.

It has been proven through numerous studies that the upconversion process from the  $T_1$  to  $S_1$  state requires TADF molecules to have a small  $\Delta E_{\text{ST}}$ , which is a fundamental requirement for achieving efficient TADF emission. The small  $\Delta E_{\text{ST}}$  can be controlled through the selection of donor and acceptor pairs and the type of connectivity between the donor and acceptor. For conjugated polymers, attention should also be paid to the triplet energy level ( $E_{\text{TS}}$ ) of the main chains, which can also affect the upconversion process of the TADF unit.

In 2016, Marc K. Etherington *et al.* demonstrated that ISC between  $^1\text{CT}$  and  $^3\text{CT}$  involves a more complex second-order

process.<sup>22</sup> This second-order process is mediated by the vibration coupling between  $^3\text{CT}$  and  $^3\text{LE}$ , which allows SOC to the  $^1\text{CT}$  state. Additionally, a reasonable energy level model was proposed, where the relative energy ordering and the energy gaps between CT and LE states [ $\Delta E(^3\text{LE}-^3\text{CT})$ ,  $\Delta E(^3\text{LE}-^1\text{CT})$ ] control the efficiencies of ISC and reverse intersystem crossing (RISC) of TADF emitters. The energy gap between  $^3\text{LE}-^3\text{CT}$  and  $^3\text{LE}-^1\text{CT}$  states serves as the key activation barrier for efficient RISC. This leads to a rapid equilibrium between the two triplet states through internal conversion, followed by coupling of  $^3\text{CT}$  to  $^1\text{CT}$  state through the second-order perturbation theory under the mediation of  $^3\text{LE}$ .

In fact, the wave function of the spin triplet state is usually not a pure  $^3\text{LE}$ , but a mixture state involving  $^3\text{CT}$  and  $^3\text{LE}$  components. Some studies have also proved that when the proportion of  $^3\text{LE}$  components is low, satisfactory  $k_{\text{RISC}}$  can also be obtained. Although the SOC is weak when the proportion of  $^3\text{LE}$  components is low, molecular vibration coupling has proved to play a key role in promoting the  $^3\text{CT}-^1\text{CT}$  transition. When the energy gap between  $^1\text{CT}$  and  $^3\text{CT}$  becomes very small, the HFC between them may become active.<sup>23</sup>

Therefore, through molecular design, adjusting the properties and energy levels of molecular excited states, and enhancing the SOC between excited states are considered to be important methods to improve the  $k_{\text{RISC}}$  of TADF materials. It is also an important strategy to improve the performance and stability of PLED devices and reduce the efficiency roll-off. However, there is also a complex relationship between the properties of TADF-conjugated polymers and their excited states. In this article, from the perspective of excited state regulation of conjugated polymers, the relationship between their molecular design, excited state properties and PLEDs performance is summarized. In addition, the molecular design and development direction of high-efficiency and high-stability PLEDs are outlined.

## 2. High-performance OLEDs with conjugated TADF polymers

### 2.1. High-efficiency

**Maintaining suitable  $\Delta E_{\text{ST}}$ .** Many studies have shown that increasing the dihedral angle between donors and acceptors

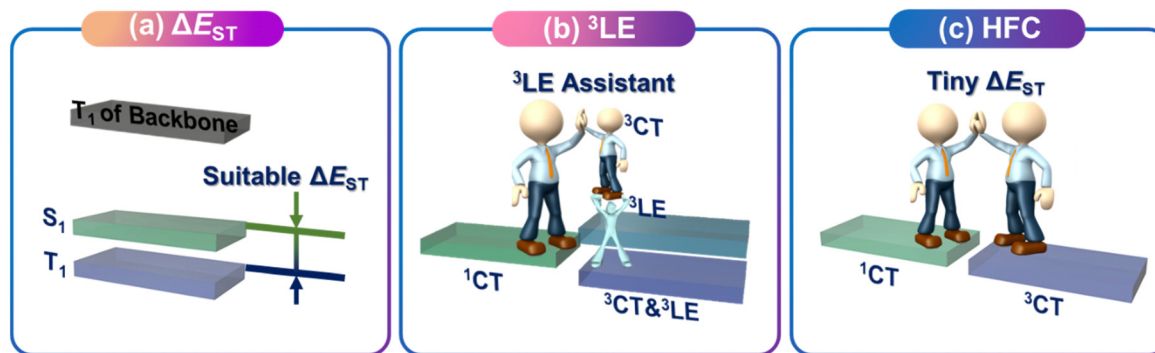


Fig. 1 The rules governing the excited state properties of conjugated polymer TADF. (a) Maintaining suitable  $\Delta E_{\text{ST}}$ ; (b) localized triplet excited state assisted reverse intersystem crossing; (c) hyperfine coupling facilitates reverse intersystem crossing.

effectively decreases the overlap between the HOMO and LUMO wavefunctions, resulting in a smaller  $\Delta E_{ST}$ .<sup>16</sup> For conjugated TADF polymers, maintaining a small  $\Delta E_{ST}$  by minimizing the influence of the polymer backbones after polymerization is a fundamental principle for the regulation of excited states. Therefore, it is necessary to have a higher energy level of the polymeric main chain than that of the emitting unit.

Common monomers used for the polymer backbones include carbazole, fluorene, diphenylthiophene, and tetramethylbenzene. They provide good carrier transport properties for conjugated polymers and promote the emission of TADF units. Fig. 2 shows some polymer structures related to suitable  $\Delta E_{ST}$ .

Because of the excellent hole-transporting ability, carbazole is a common backbone structure of conjugated polymers. The  $E_T$  of the main chain formed by the copolymerization of carbazole and other units is sufficient to satisfy most of the

visible light regions from blue-green to orange-red. Therefore, such polymers can be easily extended from small molecules and maintain a small  $\Delta E_{ST}$  without worrying about the influence of the main chain on the excited state. Recently, Yang *et al.* combined the pure carbazole backbone with multiple resonance TADF (MR-TADF) molecules to design and synthesize a series of polymers, PCzBNx.<sup>12</sup> The high  $E_T$ s of polycarbazole ensure that the extremely small  $\Delta E_{ST}$  of the side chain MR-TADF unit is not affected. And the weak electron-donating ability of carbazole will not produce long-range CT to MR-TADF units and affect the narrow emission of MR-TADF. On solution-processed OLEDs performance, PCzBN1 achieved an  $EQE_{max}$  of 17.8% and an impressive full width at half maximum (FWHM) of the electroluminescence spectrum of 27 nm. This is the first reported conjugated MR-TADF polymer, which fully demonstrates the versatility of the carbazole backbones.

Furthermore, carbazole can also work together with fluorene and tetramethylbenzene as polymeric main chains. Praetip Khammultri *et al.* designed and synthesized a series of TADF conjugated polymers (PCTXO/PCTXO-Fx (x = 25, 50, and 75)),<sup>24</sup> which possess a conjugated backbone with TPA-carbazole/fluorene moieties as the donor and a pendent 9H-thioxanthen-9-one-10,10-dioxide (TXO) as the acceptor, forming a twisted donor–acceptor structure. The  $\Delta E_{ST}$  values of four polymers are 0.15, 0.13, 0.12 and 0.12 eV, respectively, which are comparable to the  $\Delta E_{ST}$  values of the original TADF small molecule. The similar design principles have been demonstrated in the CP-PLEDs field. In 2022, two novel chiral conjugated polymers, R-P and S-P, with small  $\Delta E_{ST}$  values and thus excellent TADF properties are designed and synthesized.<sup>25</sup> A series of CP-PLEDs using R-P and S-P as light-emitting layers show  $EQE_{max}$  values of 14.9% and 15.8%, respectively. Furthermore, CP-PLEDs based on R-P and S-P present strong mirror CPEL signals at maximum emission wavelengths of 546 nm and 544 nm, respectively. The work provides a new and successful strategy for the design of chiral TADF polymers to achieve the CPEL.

However, the  $E_T$ s of the above types of carbazole backbones limit the application of blue-emitting conjugated polymers. To solve this problem, Wang *et al.* introduced tetramethylbenzene with carbazole to effectively increase the  $E_T$ s of the main chains. In 2023, poly(DOPAcDSCz-TMP), poly(DOPAcBPCz-TMP) and poly(DOPAcNICz-TMP) were designed and synthesized, in which TADF units with different electron-withdrawing abilities are located into the side chains.<sup>26</sup> The  $\Delta E_{ST}$  for all polymers is as low as 68–165 meV. The corresponding PLEDs display sky-blue, green, and red electroluminescence with  $EQE_{max}$  values of 12.5%, 16.5%, and 3.6%, respectively. The Commission Internationale de l'Eclairage (CIE) coordinates are (0.22, 0.43), (0.37, 0.57) and (0.62, 0.38), respectively. This indicates that the polymeric backbone with high triplet makes it almost applicable to TADF polymers with a full-colour spectrum except deep blue light.

Carbazole and acceptor units can also be used for the main chains of red light-emitting polymers. Wang *et al.* proposed a strategy for constructing red TADF conjugated polymers by

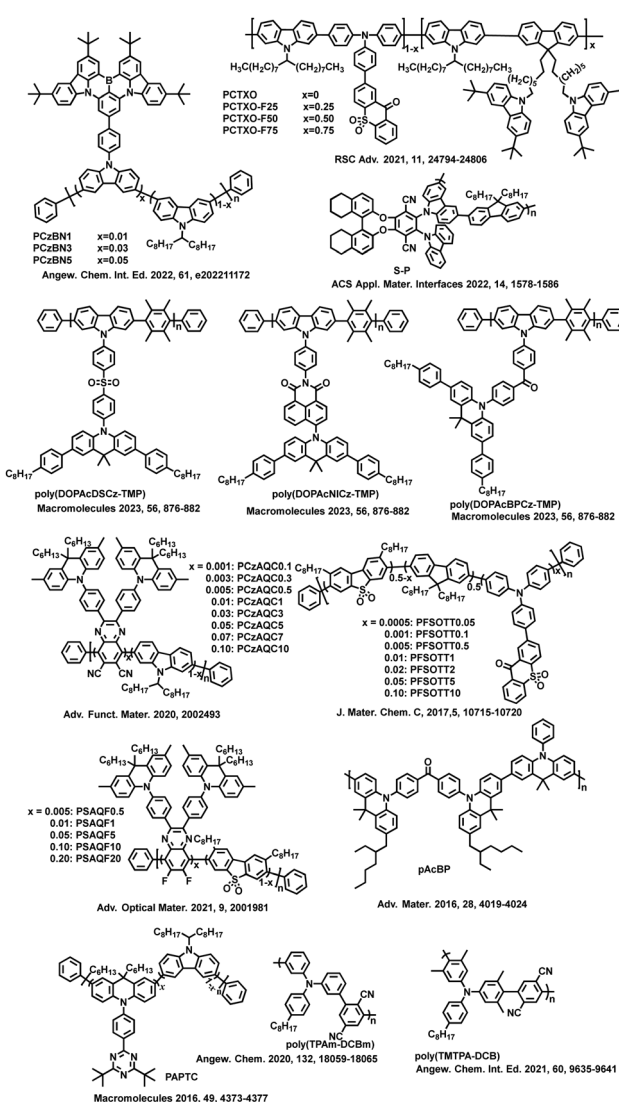


Fig. 2 Molecular structures of the selected high-efficiency TADF conjugated polymers related to suitable  $\Delta E_{ST}$ .

embedding quinoxaline-6,7-dicarbonitrile (QC) acceptors into the polycarbazole backbones and linking 9,10-dihydroacridine donors as side chains to the main chains.<sup>27</sup> Non-doped electroluminescent devices achieve an EQE<sub>max</sub> of 12.5% at 620 nm, representing the highest performance for solution-processed PLEDs based on red TADF polymers. When combining blue TADF materials and PCzAQC0.5 in a single emissive layer, bright white OLEDs with the entire visible-near infrared range (400–900 nm) are obtained with a record-high EQE<sub>max</sub> of 22.4% at this time. By further controlling the molecular weight of PCzAQC0.5, the EQE<sub>max</sub> of its red-emitting device can reach 21.2%.<sup>28</sup>

In addition to the carbazole unit as a donor, the dibenzothiophene sulfone mentioned above can also form the main chains of the conjugated polymers together with other units, for example, diphenylthiophene and fluorene. A series of conjugated polymers with the backbone-donor/pendant-acceptor architecture, PFSOTTx are designed and synthesized.<sup>29</sup> The polymers inherit the inherent TADF characteristics of small molecules. Besides, diphenylthiophene and acceptors are copolymerized to form a main chain. In 2021, a backbone-acceptor and pendant-donor TADF conjugated polymer PSAQFx is reported, which is similar to PCzAQCx but has a smaller  $\Delta E_{ST}$  and a faster  $k_{RISC}$  than PCzAQCx.<sup>13</sup> Based on PSAQFx, the doped devices achieve an EQE<sub>max</sub> of 24.8% with an emission peak at 608 nm. This is the first example of achieving EQE over 20% with an emission peak over 600 nm in TADF polymer-based OLEDs.

Molecular excited state control is closely related to the molecular structure, and it can be achieved by adjusting the structure of conjugated TADF polymers to reduce  $\Delta E_{ST}$ . For instance, optimizing the molecular excited state energy levels can be achieved by selecting appropriate donor-acceptor units and tuning the conjugation between them. In 2015, Adachi *et al.* developed a new class of conjugated polymers based on benzophenone, pCzBP and pAcBP, which consist of an alternating electron donor and acceptor unit in their main chains.<sup>30</sup> When the donor units are replaced with acridan units, the  $\Delta E_{ST}$  of the conjugated polymer decreases from 0.16 eV (pCzBP) to 0.004 eV (pAcBP). The EQE<sub>max</sub> values of OLEDs prepared *via* solution processing of the donor-acceptor polymers increase from  $8.1 \pm 0.7\%$  of pCzBP to  $9.3 \pm 0.9\%$  of pAcBP, significantly surpassing the theoretical limit of traditional fluorescent OLEDs.

In 2016, the Cheng group adjusted the  $\Delta E_{ST}$  of conjugated polymers by introducing donors into the main chains.<sup>31</sup> The carbazole and 9,10-dihydroacridine derivatives are alternately copolymerized to obtain the conjugated main chains with high  $T_1$ , in which the acceptors are either phenyl units containing electron-withdrawing cyanogen or triazine groups. The side chains are connected to the nitrogen atoms of the 9,10-dihydroacridine group at large dihedral angles, forming a twisted intramolecular charge-transfer (TICT) structure, and thus resulting in the efficient TADF conjugated polymers PAPCC and PAPTC. In PAPCC, HOMOs and LUMOs are well separated in space to achieve a smaller  $\Delta E_{ST}$ . In solution-processed PLEDs, EQE<sub>max</sub> achieves 12.6% with the emission

peak at 521 nm. This is the first report of a fully conjugated polymer with efficient TADF.

Besides, in 2020, Rao *et al.* prepared the efficient TADF polymers with a donor-acceptor conjugated structure,<sup>32</sup> in which triphenylamine (TPA) as a donor and dicyanobenzene as an acceptor are developed by changing the connection positions. When the connection position changes from the *para*-position to the *meta*-position, the  $\Delta E_{ST}$  significantly decreases from 0.44 eV to 0.10 eV due to the increased hole-electron separation. As a result, compared to the *para*-connected polymer poly(TPAp-DCBp) without TADF features, the *meta*-connected polymer poly(TPAm-DCBm) shows strong delayed fluorescence characteristics. The corresponding solution-processed OLEDs achieve an EQE of 15.4% at 532 nm. This is the first report on donor-acceptor type conjugated TADF polymers, whose performance is comparable to that of backbone-donor/pendant-acceptor and TSCT polymers. Then, they proposed a novel steric locking strategy by introducing different numbers of methyl groups into donor-acceptor conjugated polymers to obtain three polymeric emitters, poly(TPAp-DCBp), poly(DMTPA-DCB) and poly(TMTPA-DCB).<sup>16</sup> Due to the steric hindrance, the twisting angle between the donor and acceptor can be well-tuned, suppressing planar relaxation and conjugation elongation, thereby promoting hole-electron separation. Correspondingly, as the number of methyl groups increases, the twisting angle enlarges, and  $\Delta E_{ST}$  decreases from 0.44 eV to 0.22 eV and 0.09 eV, respectively. The resulting donor-acceptor conjugated polymers achieve extremely low  $\Delta E_{ST}$  (0.09 eV), enabling efficient TADF emission. The corresponding doped and undoped devices show record-high EQEs of 24.0% and 15.3%, respectively. During this period, other researchers also utilize this rule of reducing  $\Delta E_{ST}$  to report many efficient TADF conjugated polymers.

**Triplet localized excited state assisted reverse intersystem crossing.** Maintaining a small  $\Delta E_{ST}$  is a prerequisite for ensuring efficient TADF performance. Unfortunately, these papers only mention that the high device efficiency caused by smaller  $\Delta E_{ST}$  and the excited-state component types have not been analyzed. According to the El-Sayed rule, SOC is allowed between two excited states with different electronic configurations. Generally, the  $S_1$  is the  $^1CT$  state. Therefore, when the local component of  $T_1$  increases or when there exists a  $^3LE$  energy level that is closer to  $^1CT$ , it helps enhance SOC and promotes RISC. Fig. 3 shows some polymer structures related to  $^3LE$  energy level regulation.

Reineke's group reported a method for constructing TADF polymers from non-TADF units.<sup>33</sup> Due to the smaller  $\Delta E_{ST}$  of the prepared polymer P1 than the individual repeat unit and sufficiently high radiative decay rate, P1 achieves a PLQY of up to 71%. Density functional theory calculations confirm that the  $^3LE$  plays a key auxiliary role in promoting the up-conversion process, enabling the polymer to exhibit TADF properties. This work provides an encouraging strategy for producing efficient TADF oligomers and polymers from completely non-TADF units through coupling interactions. In later studies, they also reported the impact of host materials on OLEDs based on

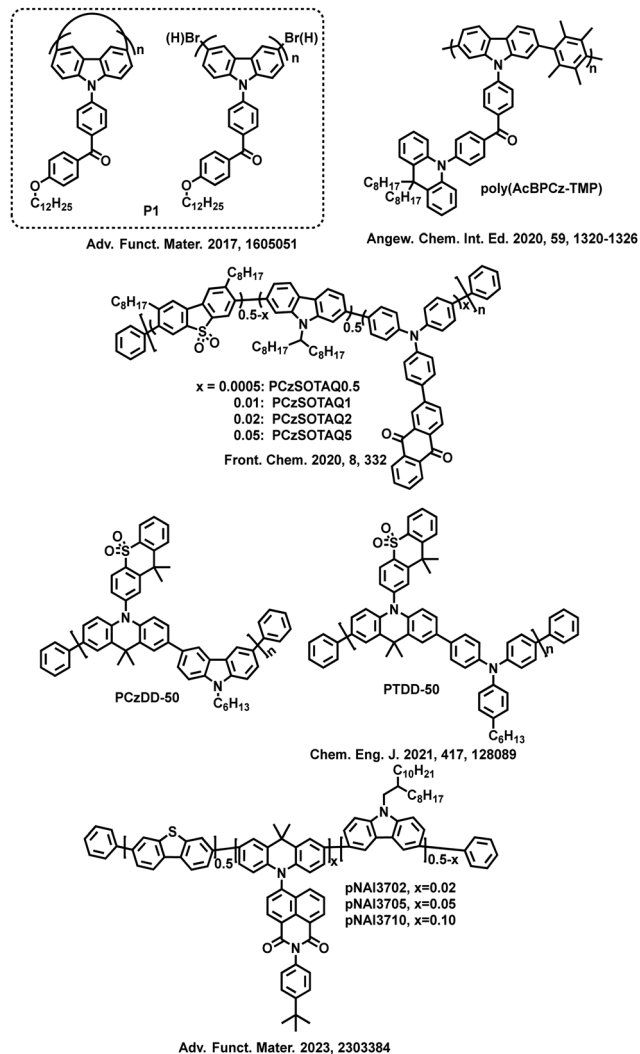


Fig. 3 Molecular structures of the selected high-efficiency TADF conjugated polymers related to  $^3\text{LE}$  assisted reverse intersystem crossing.

polymer P1.<sup>34</sup> Delayed fluorescence is hardly observed in pure films or CzSi host, but replacing the host material CzSi with mCP increases delayed fluorescence by more than three orders of magnitude. The cyan blue device based on mCP as the host material exhibits an  $\text{EQE}_{\text{max}}$  of 4.26%, while the device based on the pure P1 film displays an  $\text{EQE}_{\text{max}}$  of only 0.87%. In the context of conjugated TADF polymer based PLEDs, this work proposes that the  $^3\text{LE}$  property in polymer excited states plays an important role in achieving TADF performance. Rao *et al.* reported a “TADF + Linker” strategy, where small-molecule TADF units are coupled together through a methyl-substituted phenyl linker group (phenyl, dimethylphenyl or tetramethylphenyl) to form three different polymers, poly(AcBPCz-P), poly(AcBPCz-DMP) and poly(AcBPCz-TMP), respectively.<sup>35</sup> Analysis of the excited state energy levels for these polymers reveals that with an increase in the number of methyl groups on the linker, the CT emission (*i.e.*,  $^3\text{CT}$  and  $^1\text{CT}$ ) remains almost unchanged, but the local excited triplet ( $^3\text{LE}_b$ ) of the polymeric backbones gradually increases in energy from poly(AcBPCz-P)

to poly(AcBPCz-DMP) and poly(AcBPCz-TMP), with the  $^3\text{LE}_b$  energy level rising from 2.27 eV to 2.58 eV and 2.74 eV, respectively. The  $^3\text{LE}_b$  energy level of poly(AcBPCz-TMP) is even close to that of  $^1\text{CT}$  and  $^3\text{CT}$ . Therefore, the conjugation of the main chains could be adjusted by methyl substitution to modulate the energy levels of triplet, resulting in high-efficiency poly(AcBPCz-TMP)-based OLEDs with an EQE as high as 23.5% and CIE coordinates of (0.25, 0.52). Additionally, when combined with an orange-red TADF emitter, bright warm white electroluminescence is obtained with an  $\text{EQE}_{\text{max}}$  of 20.9% and CIE coordinates of (0.36, 0.51). The efficiencies of both monochromatic and warm white devices were the highest values reported for TADF polymers at that time. These results demonstrate the importance of the  $^3\text{LE}$  component in the auxiliary conversion process from  $^3\text{CT}$  to  $^1\text{CT}$ .

According to the second-order perturbation theory,  $^3\text{LE}$  plays an important auxiliary role in the RISC process. Two sets of conjugated polymers with anthraquinone moieties as pendant acceptors have been designed and prepared by Zhan *et al.* The acceptors are connected to the diphenylamine groups through a phenyl bridge to form TADF units, which are embedded in the polymer main chains through their donor segments, while the main chains are composed of dibenzothiophene-*S*, *S*-dioxide and 2,7-fluorene or 2,7-carbazole groups.<sup>36</sup> The model compounds 2FSO-TAQ and 2CzSO-TAQ exhibit calculated  $\Delta E_{\text{ST}}$  values of 0.20 eV and 0.16 eV, respectively, which match well with the experimental values of the polymers PFSOTAQx and PCzSOTAQx in thin films. Compared with PFSOTAQx, PCzSOTAQx exhibits a smaller  $\Delta E_{\text{ST}}$  due to the stronger electron-donating ability of the carbazole groups. Excited-state energy level information reveals that when  $\Delta E_{\text{ST}}$  is smaller ( $^1\text{CT}$  and  $^3\text{CT}$  are close), there is a  $^3\text{LE}$  component close to  $^1\text{CT}$  to assist the SOC process. Non-doped OLEDs achieve efficient red emission at 625–646 nm. When the molar content of the TADF unit is 2%, the  $\text{EQE}_{\text{max}}$  is 13.6% with CIE coordinates of (0.62, 0.37), indicating saturated red electroluminescence. Similarly, two sky-blue TADF polymer emitters, PCzDD-50 and PTDD-50 are designed and synthesized.<sup>37</sup> In these polymers, deep blue TADF molecule DMOTX-DMAC is used as a guest unit, and carbazole and triphenylamine derivatives (TPAs) are used as the host units for PCzDD-50 and PTDD-50, respectively. Molecular simulation and photophysical analysis reveal that PCzDD-50 possesses much more  $^3\text{LE}$  component in the  $T_1$  state than PTDD-50, and thus the increased  $^3\text{LE}$  component tends to promote SOC interactions between  $S_1$  and  $T_1$  according to the El-Sayed rule. Therefore, the potential enhancement of SOC interactions in PCzDD-50 can effectively accelerate the RISC process, resulting in a higher luminescence efficiency than PTDD-50. Finally, PCzDD-50 and PTDD-50 based PLEDs present  $\text{EQE}_{\text{max}}$  values of 8.2% ( $\lambda_{\text{EL}} = 488$  nm) and 5.3% ( $\lambda_{\text{EL}} = 468$  nm), respectively.

Then, pNAI37 series and pNAI28 series orange-red TADF polymers are synthesized with joint backbones of dibenzothiophene (DBT) and carbazole (Cz).<sup>38</sup> By adjusting the connecting position of the DBT unit, the polymeric performance is successfully optimized. Meanwhile, the  $^1\text{CT}$  and  $^3\text{CT}$  levels of pNAI37 series are both 17 meV higher than those of the pNAI28 series,

however, the pNAI37 series presents a smaller energy gap between the  $^1\text{CT}$  and  $^3\text{LE}$  levels [ $\Delta E(^1\text{CT}-^3\text{LE})$ ] than the pNAI28 series. Since the  $^3\text{LE}$  state can act as a medium to help excitons spin flip from triplets to singlets, a smaller  $\Delta E(^1\text{CT}-^3\text{LE})$  enables better performance due to the second-order oscillator coupling mechanism. Finally, pNAI3705 exhibits the better excited-state properties with the OLED EQE<sub>max</sub> of 20.16%, which is maintained at 10.61% at 500 cd m<sup>-2</sup>, ranking first tier among orange-red polymers. This work also demonstrates that optimizing excited-state properties by controlling the polymer chain structure is an effective way to improve device performance.

By summarizing this series of works, it is found that the properties of the excited state energy levels and the energy level differences are crucial. Specifically, according to the El-Sayed rule, when both excited states of conjugated TADF polymers display different properties (including  $^3\text{LE}$  and  $^1\text{CT}$ ),  $^3\text{LE}$  or  $^3\text{LE}_b$  can assist in completing the SOC process, achieving efficient RISC, improving the utilization efficiency of triplet excitons, and thus obtaining higher luminescence efficiency. However, it should be noted that the smaller the energy level difference between  $^1\text{CT}$  and  $^3\text{LE}$  [ $\Delta E(^1\text{CT}-^3\text{LE})$ ], the better the RISC rate.

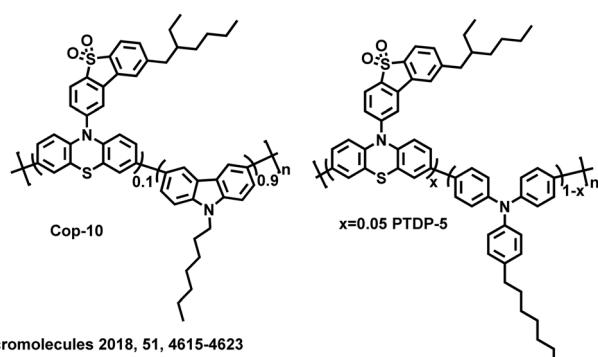
**Hyperfine coupling facilitates reverse intersystem crossing.** Another proven example of a RISC process is HFC, which occurs when the geometries of  $^1\text{CT}$  and  $^3\text{CT}$  are similar and their energy difference is very small, wherein the forbidden transitions prohibited by the El-Sayed rule can be activated due to vibrational coupling. Molecular structures of the selected high-efficiency TADF conjugated polymers related to HFC are shown in Fig. 4.

For example, the carbazole derivatives are combined with TADF unit, 2-(10H-phenothiazin-10-yl)dibenzothiophene-S,S-dioxide (DBTO2-PTZ) to construct three conjugated polymers, Homo, Cop-50 and Cop-10.<sup>39</sup> The results show that the content of carbazole derivative units not only effectively suppresses the exciton annihilation and non-radiative transitions but also manipulates the molecular orbital distribution and  $\Delta E_{\text{ST}}$  value, and even regulates the properties of excited states. Through the analysis of natural transition orbitals (NTOs) of the three

polymers, it is concluded that although RISC between  $^1\text{CT}$  and  $^3\text{CT}$  may be inhibited due to weak SOC according to the El-Sayed rule, under certain conditions, RISC can also be achieved between  $^1\text{CT}$  and  $^3\text{CT}$ , which is attributed to the HFC of spins.<sup>40,41</sup> Therefore, rational control of excited state properties may help guide the synthesis of efficient TADF polymers. Among the three polymers, COP-10 exhibits a higher  $k_{\text{RISC}}$  and PLQY in the thin film state. The optimized OLEDs achieve an EQE<sub>max</sub> of 15.7% with a turn-on voltage of only 3.2 V. Then, two double-emissive TADF polymers PTDP-5 and PTDP-10 are reported by replacing the carbazole derivatives on the polymeric main chains with TPAs,<sup>42</sup> in which TPAs served as the main chains and blue emitters, while the alkylated TADF small molecules (DBTO2-PTZ) served as orange-yellow emitters. Due to the strong fluorescent emission characteristics and non-planar structure of TPAs in the main chains of TADF polymers, double-emissive polymers have been obtained by utilizing the emission of TPAs and DBTO2-PTZ TADF units. Increasing the proportion of TPA units enhances the relative intensity of blue emission. Therefore, in solution-processed OLEDs, as the percentage of TPAs units in the polymeric main chain increases, not only the CIE coordinates of PTDP-10 shift from (0.44, 0.43) to (0.38, 0.35) of PTDP-5, achieving warm-white emission, but also the EQE<sub>max</sub> value increases from 4.8% of PTDP-10 to 7.1% of PTDP-5. The excited-state characteristics of the two polymers, PTDP-5 and PTDP-10, are also analyzed and found to follow the same rules as COP-10. It is shown that if the two excited states have the same properties ( $^3\text{CT}$  and  $^1\text{CT}$ ), the RISC between  $^1\text{CT}$  and  $^3\text{CT}$  may be suppressed due to weak SOC. However, when the energy level difference between  $^3\text{CT}$  and  $^1\text{CT}$  is very small, the HFC can be activated to break the El-Sayed rule, achieving upconversion and thus improving device performance. The OLED performance and the excited state energy levels of the selected TADF conjugated polymers with high efficiency are summarized in Table 1.

## 2.2. The efficiency roll-offs

The high efficiency roll-off is one of the main reasons for limiting the commercial application of TADF materials. Conjugated polymers have unique advantages in solving the efficiency roll-off of OLEDs. On one hand,  $\pi$ -conjugated TADF polymers display the advantageous charge transporting properties derived from the delocalized  $\pi$ -electron bonding along the polymeric backbones. That is to say, the bonding and antibonding orbitals can form the delocalized valence and the conduction wavefunctions, which can provide a channel for mobile charge carriers and thus suppress the exciton concentration quenching.<sup>43</sup> On the other hand, TADF chromophores are sparsely embedded in the polymeric backbones and separated by a “blocking segment” formed by the host oligomer with higher triplet over a sufficiently long distance, thereby preventing short-range Dexter energy transfer. From this viewpoint, the conjugated TADF polymers are a potential candidate for fabricating PLEDs with suppressive efficiency roll-off resulting from the unbalanced charge transportation and the high exciton concentration. All of these conjugated polymers present the low



Macromolecules 2018, 51, 4615-4623

ACS Appl. Polym. Mater. 2019, 1, 2204-2212

Fig. 4 Molecular structures of the selected high-efficiency TADF conjugated polymers related to HFC.

Table 1 OLED performance and excited state energy levels of the selected high-efficiency TADF conjugated polymers

Polymers	$k_{\text{RISC}}$ ( $10^5$ s $^{-1}$ )	$\Delta E_{\text{ST(exp)}}$ (eV)	$\Delta E_{\text{ST(cal)}}$ <sup>b</sup> (eV)	$\lambda_{\text{EL}}$ <sup>c</sup> (nm)/CIE	EQE <sup>d</sup> (%)	Type <sup>e</sup>	Ref.
pAcBP	1.3	0.10	0.004	548/(0.38, 0.57)	9.30	$\Delta E_{\text{ST}}$	30
PAPTC	—	0.13	0.14	521/(0.30, 0.59)	12.6	$\Delta E_{\text{ST}}$	31
PFSOTT2	—	0.26	0.09	406, 566/(0.42, 0.45)	9.90	$\Delta E_{\text{ST}}$	29
PFSOTT2	—	0.26	0.09	592/(0.51, 0.47)	19.4	$\Delta E_{\text{ST}}$	29
P1	—	0.023	0.12	480/(0.24, 0.37)	4.30	<sup>3</sup> LE	34
Cop-10	14.4	0.043	0.022	578/(0.46, 0.49)	15.7	HFC	39
PTDP-5	0.14	0.060	—	428, 600/(0.38, 0.35)	7.10	HFC	42
Poly(AcBPCz-TMP)	—	0.12	0.19	507/(0.25, 0.52)	23.5	<sup>3</sup> LE <sub>b</sub>	35
Poly(AcBPCz-TMP)	—	0.12	0.19	510, 552/(0.36, 0.51)	20.9	<sup>3</sup> LE <sub>b</sub>	35
PCzDD-50	2.00	0.042	1.00	488/(0.22, 0.35)	8.20	<sup>3</sup> LE	37
PTDD-50	1.12	0.047	0.86	468/(0.17, 0.22)	5.30	<sup>3</sup> LE	37
PNAI3705	7.20	0.04	0.008	610/(0.57, 0.38)	20.16	<sup>3</sup> LE	38
PCzSOTAQ2	—	0.12	0.16	642/(0.62, 0.37)	13.6	<sup>3</sup> LE	36
PCzAQCO.5	2.90	0.18	0.18	620/(0.56, 0.42)	12.5	$\Delta E_{\text{ST}}$	27
PCzAQCO.5	2.90	0.18	0.18	454, 632/(0.52, 0.38)	22.4	$\Delta E_{\text{ST}}$	27
PSAQF10	8.60	0.20	0.05	608/(0.48, 0.49)	24.8	$\Delta E_{\text{ST}}$	13
Poly(TPAm-DCBm)	1.01	0.10	0.16	532/(0.34, 0.57)	15.4	$\Delta E_{\text{ST}}$	32
poly(TMTPA-DCB)	3.53	0.09	0.08	532/(0.34, 0.57)	24.0	$\Delta E_{\text{ST}}$	16
PCTXO-F75	—	0.12	—	611/(0.55, 0.44)	1.54	$\Delta E_{\text{ST}}$	24
PCTXO	—	0.15	—	603/(0.56, 0.43)	10.4	$\Delta E_{\text{ST}}$	24
poly(DOPAcDSCz-TMP)	3.23	0.17	0.01	488/(0.22, 0.43)	12.5	$\Delta E_{\text{ST}}$	26
poly(DOPAcBPCz-TMP)	21.5	0.07	0.006	530/(0.37, 0.57)	16.5	$\Delta E_{\text{ST}}$	26
poly(DOPAcNICz-TMP)	13.5	0.07	0.007	620/(0.62, 0.38)	3.60	$\Delta E_{\text{ST}}$	26
R-P	6.28	0.045	0.047	546/(0.41, 0.57)	14.9	$\Delta E_{\text{ST}}$	25
S-P	6.31	0.061	0.047	544/(0.40, 0.57)	15.8	$\Delta E_{\text{ST}}$	25

<sup>a</sup> Calculated from fluorescence and phosphorescence spectra. <sup>b</sup> Calculated by TD-DFT at the B3LYP/6-31G(d,p) level. <sup>c</sup> Commission Internationale de l'Eclairage (CIE) coordinates. <sup>d</sup> The maximum EQE. <sup>e</sup>  $\Delta E_{\text{ST}}$ , <sup>3</sup>LE, <sup>3</sup>LE<sub>b</sub> and HFC represent the strategy of controlling suitable  $\Delta E_{\text{ST}}$ , triplet localized excited state, triplet localized excited state of main chains, and hyperfine coupling assisted reverse intersystem crossing, respectively.

efficiency roll-off and small  $\Delta E_{\text{ST}}$ . However, there are very few studies on the regulation of the excited state. The research studies focus on separating HOMO and LUMO distribution in order to reduce  $\Delta E_{\text{ST}}$ , and thus improve  $k_{\text{RISC}}$ , which would reduce the concentration of triplet excitons to suppress concentration quenching, thereby achieving a lower efficiency roll-off. The molecular structures of the selected TADF conjugated polymers with low efficiency roll-off are shown in Fig. 5. The OLED performance and the excited state energy levels of the selected TADF conjugated polymers with low efficiency roll-off are summarized in Table 2.

From 2017 to 2018, a series of studies on the conjugated polymers with low efficiency roll-off were conducted by Cheng and co-workers.<sup>44–48</sup> These polymers have an identical backbone consisting of 3,6-carbazolyl and 2,7-acridinyl rings. One acridine ring and each acceptor group pendant constitute a definite TADF unit with the twisted donor–acceptor structure, which is incorporated into the polymeric main chains through 2,7-position of the acridine ring with the varied contents.

With the development of study on the conjugated TADF polymers, since 2020, our group has reported several TADF conjugated polymer-based OLEDs with low efficiency roll-off. In 2020, we designed and synthesized the fluorinated and chlorinated  $\pi$ -conjugated TADF polymers and their non-halogenated analogues, respectively.<sup>49</sup> The halogenation can aggrandize the <sup>3</sup>LE component of  $T_1$ , which is favourable to enhancing SOC and RISC processes. Eventually, the halogenated emitter-based PLEDs can reach a high EQE<sub>max</sub> of over 20%, and extremely low efficiency roll-off sustaining over 18% EQE at a luminance of 1000 cd m $^{-2}$ . This study opens a way to design high-efficiency

TADF materials by halogenation and thus guides the future research on the high-performance PLEDs. The excited states of halogenated TADF polymers also abide by the El-Sayed rule, wherein the  $S_1$  and  $T_1$  states featuring the different excited natures generally possess the impressive SOC matrix element values. The auxiliary role of <sup>3</sup>LE in the excited state for RISC is proved again.

Besides, some studies have shown that when  $S_1$  and  $T_1$  have the same excited state properties, in some specific cases, lower efficiency roll-off can also be obtained. On one hand, Yersin *et al.* recently demonstrated that the RISC process with a minimal  $\Delta E_{\text{ST}}$ , extremely similar geometries, and energetically nearby lying states for SOC and configuration interaction can be carried out quickly *via* vibronic coupling between the lowest <sup>1</sup>CT and <sup>3</sup>CT states.<sup>21</sup> This rule has also been proven by our newly prepared TADF conjugated polymer pBP-PXZ.<sup>50</sup> pBP-PXZ shows the close energy levels of <sup>1</sup>CT and <sup>3</sup>CT, moreover, <sup>1</sup>CT and <sup>3</sup>CT have extremely similar geometries, negligible  $\Delta E(^1\text{CT}-^3\text{CT})$  (8 meV), and with a high proportion of <sup>3</sup>LE features in  $T_2$ . With the assistance of <sup>3</sup>LE, pBP-PXZ can complete the rapid RISC process. Finally, the EQE<sub>max</sub> of OLEDs based on pBP-PXZ neat films is 13.71%. Even the OLEDs based on pBP-PXZ-doped films can achieve an EQE<sub>max</sub> of 23.11%, exhibiting no roll-off when the luminance is less than 200 cd m $^{-2}$  and show only a 3% EQE decrease at 500 cd m $^{-2}$ . The EQE remains above 19% under 1000 cd m $^{-2}$ , which is the highest device efficiency among TADF polymer-based OLEDs under high luminance. On the other hand, Serdiuk *et al.* have recently demonstrated that the activated SOC by molecular vibrations plays a key role in facilitating direct RISC with a

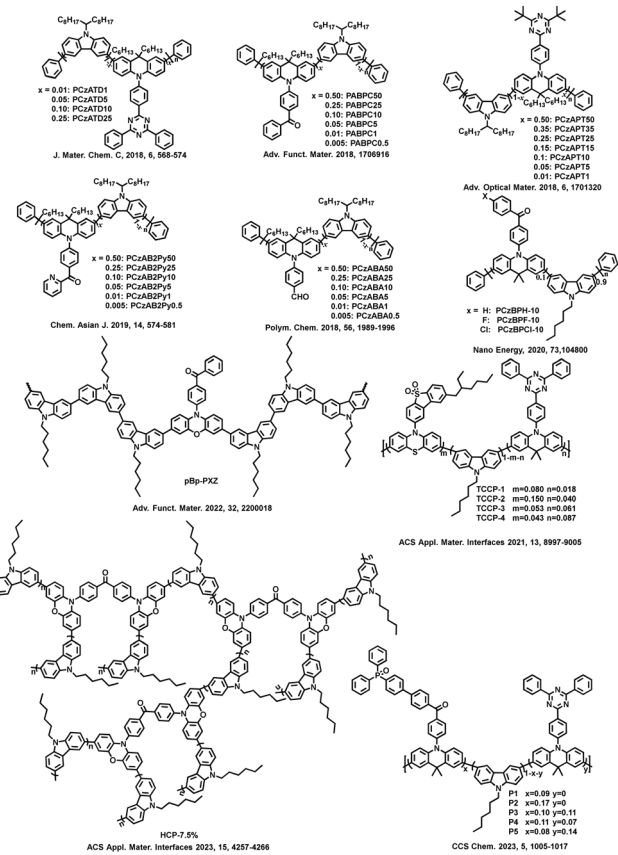


Fig. 5 Molecular structures of the selected TADF conjugated polymers with low efficiency roll-off.

high rate of  $^3\text{CT}$ – $^1\text{CT}$  transition *via* the same CT states of different multiplicities.<sup>23</sup> We also confirmed that the similar molecular vibrations and electronic structures between  $^1\text{CT}$  and  $^3\text{CT}$  states could minimize reorganization energy in the hyperbranched conjugated polymer (HCPs) system.<sup>51</sup> The RISC process can be performed quickly *via* vibronic coupling between the lowest  $^1\text{CT}$  and  $^3\text{CT}$  states with a minimal  $\Delta E_{\text{ST}}$ , extremely similar geometries, and energetically nearby lying states. Accordingly,

the transitions forbidden by the El-Sayed rule can be activated due to vibrational coupling perturbations. Especially, the degenerated states of the HCPs with D–A–D type TADF characteristics would be strongly coupled owing to their energetic proximity and establish a multiple-CT vibrationally enhanced SOC for a fast RISC. Coupling with the efficient energy transfer process generated by advantageous structural features of HCPs, the strongly electron-withdrawing oxygen atoms located on the TADF cores further accelerate hole transportation from the host chains to the TADF cores. Under a rational regulation of the TADF core ratio, the related non-doped red-emitting device performs an outstanding performance with an  $\text{EQE}_{\text{max}}$  of 8.39% and exhibits no roll-off while the luminance is less than  $100 \text{ cd m}^{-2}$  and only 3.3% decrease at  $500 \text{ cd m}^{-2}$ . Simultaneously, the EQE can be maintained at 7.4% under  $1000 \text{ cd m}^{-2}$ .

As mentioned earlier, the TADF conjugated polymers can be directly used as light-emitting layers of PLEDs. In order to further improve device performance, the TADF polymer can also be used as the host material in host–guest PLEDs to suppress triplet–triplet annihilation. Based on the existing works,<sup>52–54</sup> it can be concluded that the  $E_{\text{TS}}$  of the conjugated polymer must be higher than that of the guest TADF material to prevent energy backflow from the guest material to the host material. From the perspective of regulating excited state energy levels, in order to achieve low efficiency roll-off, researchers have developed TADF sensitizers. TADF sensitizers have a high  $k_{\text{RISC}}$  and can transfer the singlet excitons in the sensitizer unit through Förster resonance energy transfer to the singlet excitons of the emitter unit, thus avoiding the inefficient RISC process of the emitter itself. It is easy to understand that traditional intermolecular sensitization (IMS) strategies are prone to phase separation between the TADF sensitizer and the emitter. In this case, our group proposed a new intramolecular sensitization strategy by covalently binding the TADF sensitizer to the conjugated polymer luminescent material.<sup>55</sup> By properly adjusting the ratio of the sensitizer and luminescent unit in the polymer, the intramolecular sensitized conjugated TADF polymer TCCP-3 is obtained, with a  $k_{\text{RISC}}$  value greater than  $10^6 \text{ s}^{-1}$  and simultaneously suppressing the

Table 2 OLED performance and excited state energy levels of the selected TADF conjugated polymers with low efficiency roll-off

Polymers	CIE <sup>a</sup> / $\lambda_{\text{EL}}$ (nm)	EQE (%)						Ref.
		Maximum values	1000 cd m <sup>-2</sup>	Roll-off <sup>b</sup>	$\Delta E_{\text{ST}}^c$	Type <sup>d</sup>		
PCzATD5	(0.41, 0.55)/560	15.5	14.5	6.45	0.09	$\Delta E_{\text{ST}}$	44	
PABPC5	(0.40, 0.56)/545	18.1	17.8	1.66	0.12	$\Delta E_{\text{ST}}$	45	
PCzAPT10	(0.36, 0.55)/-	16.9	15.6	7.69	—	$\Delta E_{\text{ST}}$	46	
PCzAB2Py5	(0.48, 0.51)/573	11.9	11.3	5.04	0.10	$\Delta E_{\text{ST}}$	47	
PCzABA10	(0.39, 0.57)/545	10.6	10.3	2.83	0.22	$\Delta E_{\text{ST}}$	48	
PCzBPF-10	(0.38, 0.56)/542	20.0	18.2	9.00	0.01	$^3\text{LE}$	49	
pBP-PXZ	(0.52, 0.48)/584	13.7	8.86	35.4	0.028	$^3\text{LE}$	50	
HCP-7.5%	(0.55, 0.45)/600	8.39	7.43	11.4	0.038	VC	51	
TCCP-3	(0.34, 0.54)/535	17.8	16.0	10.1	0.017	IMS	55	
P5	(0.42, 0.55)/553	25.4	24.2	4.72	0.007	IMS	9	

<sup>a</sup> Commission Internationale de l'Eclairage (CIE) coordinates. <sup>b</sup> The roll-off value with respect to the maximum EQE. <sup>c</sup> Measured in toluene solution.  $\Delta E_{\text{ST}} = E_{\text{S}} - E_{\text{T}}$ . <sup>d</sup>  $\Delta E_{\text{ST}}$ ,  $^3\text{LE}$ , VC and IMS represent the strategy of controlling suitable  $\Delta E_{\text{ST}}$ , triplet localized excited state, vibronic coupling and intermolecular sensitization assisted reverse intersystem crossing, respectively.

non-radiative transition of triplet excitons. Therefore, its PLQY can reach nearly 90%. The EQE<sub>max</sub> of the solution-processed OLEDs reaches 17.8% with extremely low efficiency roll-off. Subsequently, we modified the light-emitting TADF unit with the electron-transporting material triphenylphosphine oxide to achieve the balanced charge carrier transport.<sup>9</sup> By carefully adjusting the proportions of each components, we obtained P1-P5, among which P5 demonstrates a remarkable PLQY up to 90% and an exceptionally high  $k_{RISC}$  of  $3 \times 10^6 \text{ s}^{-1}$ . The solution-processed PLEDs exhibit an EQE value of 25.4% with an emission peak at approximately 550 nm, representing record-breaking high-performance PLEDs. Additionally, significant suppression of efficiency roll-off was achieved, maintaining an EQE value of 24.2% at 1000 cd m<sup>-2</sup>, with the efficiency roll-off below 5%. This work provides an effective strategy for achieving high EQE and low efficiency roll-off. The energy transfer path of the excited state in the intramolecular sensitization strategy is shown in Fig. 6. These results demonstrate the importance of the intramolecular sensitization strategy in designing highly efficient conjugated TADF polymer emitters in molecular electronics.

After reviewing the regulation of the excited state energy level in high efficiency and low efficiency roll-off conjugated TADF polymers, it was found that the regulations were basically consistent. In fact, both high efficiency and low efficiency roll-off are important performance indicators for evaluating PLEDs, and they are inseparable and complementary in applications. Therefore, by carefully designing materials with appropriate excited state energy levels, both high efficiency and low efficiency roll-off can be achieved, simultaneously. In order to compare the performance of the reviewed TADF conjugated polymers, we summarize the OLED efficiency of TADF polymers based on the emission colour as shown in Fig. 7. As shown in Fig. 7, green TADF conjugated polymers have the most abundant types and highest efficiency, and the types of red TADF conjugated polymers need to be further enriched. Importantly, it is quite difficult to gain conjugated TADF polymers with blue and even deep-blue emissions, due to the limitation of the  $E_{TS}$  of the main chains. Currently, the bluest TADF-conjugated polymer, PTDD-50, shows only sky-blue emission.

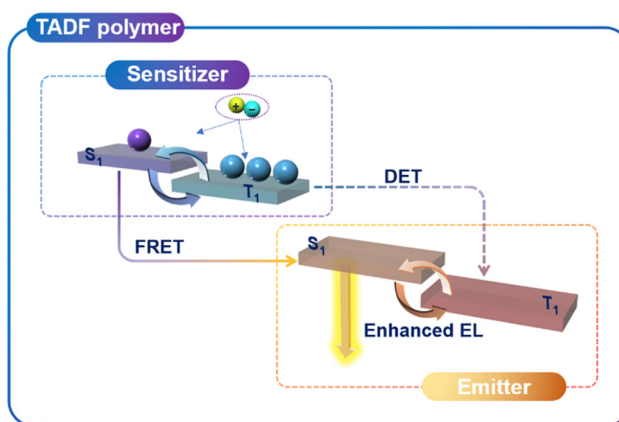


Fig. 6 The energy transfer path of the excited state in the intramolecular sensitization strategy.

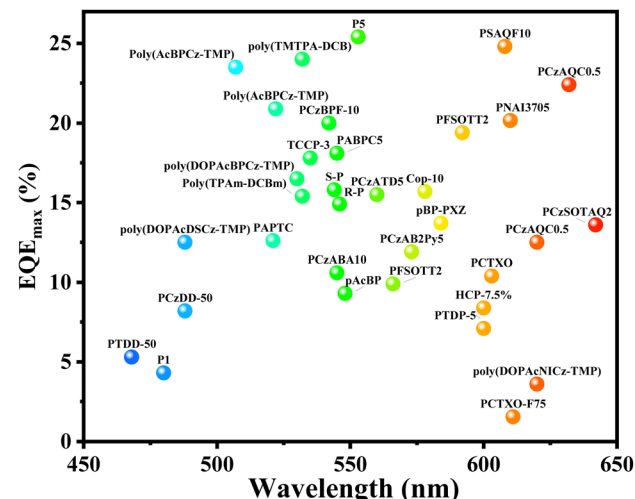


Fig. 7 The performance of the reviewed TADF conjugated polymers.

### 3. Summary and outlook

From the perspective of the method of characterizing the excited state, the excited state properties and data of the TADF conjugated polymers discussed in this article are obtained through experiments and time-dependent density functional theory (TD-DFT) calculations. We summarize these two methods. On the one hand, researchers can obtain information about S<sub>1</sub> and T<sub>1</sub> through experiments. S<sub>1</sub> and T<sub>1</sub> energy levels of polymers can be determined by the onset positions of the fluorescence spectra and the phosphorescence spectra at 77 K, respectively. On the other hand, the nature of excited states is obtained through TD-DFT calculations. DFT is the standard computational method for studying the photophysical properties of TADF emitters. It is widely used to guide molecular design and provide a deeper understanding of the TADF mechanism. Traditional hybrid functionals, especially B3LYP,<sup>56</sup> PBE0,<sup>57</sup> and distance-corrected functionals such as omega-tuned LC $\omega$ PBE,<sup>58</sup> have become the most popular methods in TADF studies. For D-A type TADF emitters, these methods usually predict S<sub>1</sub>/T<sub>1</sub>/T<sub>2</sub> properties, energy level gap, and  $\Delta E_{ST}$  values with good agreement with experimental results. It is worth noting that most reports to date have only discussed ground-state DFT calculations, with few providing time-dependent DFT results. To address this modelling problem for TADF emitters, some theoretical papers have emerged.<sup>59</sup> With the continuous application of artificial intelligence in various aspects of our lives and the development of quantum chemistry calculations, it is hoped that more model research achievements applied to the theoretical calculation of TADF emitters will emerge, providing researchers with theoretical simulation results closer to experimental values. In addition, in the future, finely tuned material excited state properties can be achieved through computer-aided simulations to design and screen for more efficient TADF molecules, replacing the method of synthesizing a series of emitters and then screening for the most efficient ones, which has high time and economic costs.

From the perspective of regulating the excited states of conjugated TADF polymers, it is necessary to minimize the  $\Delta E_{ST}$  between  $S_1$  and  $T_1$  to ensure effective RISC, which depends on the separation of HOMOs and LUMOs. Therefore, in the early days, the most common design strategy for TADF materials was based on highly twisted (or nearly orthogonal) donor-acceptor structures with strong ICT characteristics to fully separate the spatial distribution of these frontier orbitals. Following this basic principle of regulating excited states, reducing the  $\Delta E_{ST}$  of conjugated TADF polymers has led to significant progress in the development of efficient TADF materials. As research continues to deepen, researchers have begun to look for rules for regulating excited state energy levels by manipulating the excited state natures and energy gaps of luminescent materials. Based on a review of the excited-state energy level information of the existing high-performance conjugated polymer electroluminescent materials, it is concluded that excited states have different properties ( $^1CT$  and  $^3LE$ ), and the  $^3LE$  state assists in completing the SOC process during the efficient thermal conversion of  $T_1$  into  $S_1$ . Additionally, the energy gap between  $^3LE$  and  $^1CT$  is more important, as a smaller value helps ensure rapid RISC and high efficiency devices. If the excited states have the same properties ( $^1CT$  and  $^3CT$ ), then the energy gap between  $^3CT$  and  $^1CT$  becomes more important because when this value is small enough, it can break the El-Sayed forbidden  $^3CT$ – $^1CT$  transition, achieving upconversion. Of course, the regulation of excited states in conjugated TADF polymers is not limited to these rules, and there are many deeper rules worth exploring for researchers.

From the perspective of molecular design, the high  $E_{TS}$  of polymeric main chains are an important factor to ensure the suitable  $\Delta E_{ST}$  of TADF conjugated polymers. Common host units include carbazole, fluorene, diphenylthiophene, tetramethylbenzene and so on. A suitable  $\Delta E_{ST}$  for TADF conjugated polymers can be achieved by selecting appropriate donor-acceptor units and tuning the conjugation between them. For example, steric hindrance is introduced to adjust the twisting angle between the donor and acceptor. Besides, by summarizing the molecular structures of the selected high-efficiency TADF conjugated polymers related to  $^3LE$  assisted RISC and related to HFC, we found that the copolymerization of carbazole/carbazole derivatives with donors of TADF units as polymeric main chains might be a general molecular design strategy. Surprisingly, TADF conjugated polymers with low efficiency roll-off also follow this strategy.

Indeed, achieving high efficiency and low roll-off simultaneously is a major challenge faced by TADF conjugated polymers and is also the direction for future development. To achieve this, researchers will need to continue developing new design strategies and exploring more in-depth rules for regulating excited-state properties. Additionally, further advancements in theoretical modelling and simulation techniques could help researchers predict the performance of TADF materials more accurately before they are synthesized, saving time and resources. Overall, the goal is to develop TADF materials that can be used in a wide range of applications,

from displays and lighting to sensing and biomedical imaging, providing a more sustainable and cost-effective alternative to traditional optoelectronic materials.

## Author contributions

Maoqiu Li: writing – original draft and editing; Lei Hua: figure editing; Junteng Liu: investigation and supervision; Zhongjie Ren: manuscript revision and supervision.

## Conflicts of interest

There are no conflicts to declare.

## Acknowledgements

We acknowledge the financial support from the National Natural Science Foundation of China (No. 52273164) and the Shandong Provincial Natural Science Foundation (ZR2022ZD37).

## References

- 1 G. Hong, X. Gan, C. Leonhardt, Z. Zhang, J. Seibert, J. M. Busch, S. Bräse and A. Brief, History of OLEDs-Emitter Development and Industry Milestones, *Adv. Mater.*, 2021, **33**, e2005630.
- 2 H. Fu, Y.-M. Cheng, P.-T. Chou and Y. Chi, Feeling blue? Blue phosphors for OLEDs, *Mater. Today*, 2011, **14**, 472–479.
- 3 X. Cai and S.-J. Su, Marching Toward Highly Efficient, Pure-Blue, and Stable Thermally Activated Delayed Fluorescent Organic Light-Emitting Diodes, *Adv. Funct. Mater.*, 2018, **28**, 1802558.
- 4 J. H. Burroughes, D. D. C. Bradley, A. R. Brown, R. N. Marks, K. Mackay, R. H. Friend, P. L. Burns and A. B. Holmes, Light-emitting diodes based on conjugated polymers, *Nature*, 1990, **347**, 539–541.
- 5 L. Hua, S.-k Yan and Z.-j Ren, Molecular Design and Device Performance of Thermally Activated Delayed Fluorescent Polymer Materials, *Acta Polym. Sin.*, 2020, **51**, 457.
- 6 Q. Zhang, J. Li, K. Shizu, S. Huang, S. Hirata, H. Miyazaki and C. Adachi, Design of efficient thermally activated delayed fluorescence materials for pure blue organic light emitting diodes, *J. Am. Chem. Soc.*, 2012, **134**, 14706–14709.
- 7 Y. Liu, C. Li, Z. Ren, S. Yan and M. R. Bryce, All-organic thermally activated delayed fluorescence materials for organic light-emitting diodes, *Nat. Rev. Mater.*, 2018, **3**, 18020.
- 8 Q. Zhang, B. Li, S. Huang, H. Nomura, H. Tanaka and C. Adachi, Efficient blue organic light-emitting diodes employing thermally activated delayed fluorescence, *Nat. Photonics*, 2014, **8**, 326–332.
- 9 Y. Liu, Y. Xie, L. Hua, X. Tong, S. Ying, Z. Ren and S. Yan, Realizing External Quantum Efficiency over 25% with Low Efficiency Roll-Off in Polymer-Based Light-Emitting Diodes Synergistically Utilizing Intramolecular Sensitization and

Bipolar Thermally Activated Delayed Fluorescence Monomer, *CCS Chem.*, 2022, **5**, 1005–1017.

10 J. Hu, Q. Li, X. Wang, S. Shao, L. Wang, X. Jing and F. Wang, Developing Through-Space Charge Transfer Polymers as a General Approach to Realize Full-Color and White Emission with Thermally Activated Delayed Fluorescence, *Angew. Chem., Int. Ed.*, 2019, **58**, 8405–8409.

11 C. Li, A. K. Harrison, Y. Liu, Z. Zhao, F. B. Dias, C. Zeng, S. Yan, M. R. Bryce and Z. Ren, TADF dendronized polymer with vibrationally enhanced direct spin-flip between charge-transfer states for efficient non-doped solution-processed OLEDs, *Chem. Eng. J.*, 2022, **435**, 134924.

12 T. Wang, Y. Zou, Z. Huang, N. Li, J. Miao and C. Yang, Narrowband Emissive TADF Conjugated Polymers towards Highly Efficient Solution-Processible OLEDs, *Angew. Chem., Int. Ed.*, 2022, **61**, e202211172.

13 T. Wang, B. Yao, K. Li, Y. Chen, H. Zhan, X. Yi, Z. Xie and Y. Cheng, Backbone-Acceptor/Pendant-Donor Strategy for Efficient Thermally Activated Delayed Fluorescence Conjugated Polymers with External Quantum Efficiency Close to 25% and Emission Peak at 608 nm, *Adv. Opt. Mater.*, 2021, **9**, 2001981.

14 K.-C. Pan, S.-W. Li, Y.-Y. Ho, Y.-J. Shiu, W.-L. Tsai, M. Jiao, W.-K. Lee, C.-C. Wu, C.-L. Chung, T. Chatterjee, Y.-S. Li, K.-T. Wong, H.-C. Hu, C.-C. Chen and M.-T. Lee, Efficient and Tunable Thermally Activated Delayed Fluorescence Emitters Having Orientation-Adjustable CN-Substituted Pyridine and Pyrimidine Acceptor Units, *Adv. Funct. Mater.*, 2016, **26**, 7560–7571.

15 Z. Zhao, S. Yan and Z. Ren, Regulating the Nature of Triplet Excited States of Thermally Activated Delayed Fluorescence Emitters, *Acc. Chem. Res.*, 2023, **56**, 1942–1952.

16 J. Rao, L. Yang, X. Li, L. Zhao, S. Wang, H. Tian, J. Ding and L. Wang, Sterically-Locked Donor-Acceptor Conjugated Polymers Showing Efficient Thermally Activated Delayed Fluorescence, *Angew. Chem., Int. Ed.*, 2021, **60**, 9635–9641.

17 Y. Jiang, P. Lv, J. Q. Pan, Y. Li, H. Lin, X. W. Zhang, J. Wang, Y. Y. Liu, Q. Wei, G. C. Xing, W. Y. Lai and W. Huang, Low-Threshold Organic Semiconductor Lasers with the Aid of Phosphorescent Ir(III) Complexes as Triplet Sensitizers, *Adv. Funct. Mater.*, 2019, **29**, 1806719.

18 Z. Huang, H. Xie, J. Miao, Y. Wei, Y. Zou, T. Hua, X. Cao and C. Yang, Charge Transfer Excited State Promoted Multiple Resonance Delayed Fluorescence Emitter for High-Performance Narrowband Electroluminescence, *J. Am. Chem. Soc.*, 2023, **145**, 12550–12560.

19 R. S. Nobuyasu, Z. Ren, G. C. Griffiths, A. S. Batsanov, P. Data, S. Yan, A. P. Monkman and M. R. Bryce, a.D.F. B., Rational Design of TADF Polymers using a DA Monomer with Enhanced TADF Efficiency induced by the Energy Alignment of Charge Transfer and Local Triplet Excited States, *Adv. Opt. Mater.*, 2015, **4**, 597–607.

20 F. B. Dias, S. Pollock, G. Hedley, L.-O. Pålsson and A. Monkman, Intramolecular Charge Transfer Assisted by Conformational Changes in the Excited State of Fluorene-dibenzothiophene-S,S-dioxide Co-oligomers, *J. Phys. Chem. B*, 2006, **110**, 19329–19339.

21 H. Yersin, L. Mataranga-Popa, R. Czerwieniec and Y. Dovbii, Design of a New Mechanism beyond Thermally Activated Delayed Fluorescence toward Fourth Generation Organic Light Emitting Diodes, *Chem. Mater.*, 2019, **31**, 6110–6116.

22 M. K. Etherington, J. Gibson, H. F. Higginbotham, T. J. Penfold and A. P. Monkman, Revealing the spin-vibronic coupling mechanism of thermally activated delayed fluorescence, *Nat. Commun.*, 2016, **7**, 1–7.

23 I. E. Serdiuk, M. Monka, K. Kozakiewicz, B. Liberek, P. Bojarski and S. Y. Park, vibrationally Assisted Direct Intersystem Crossing between the Same Charge-Transfer States for Thermally Activated Delayed Fluorescence: Analysis by Marcus-Hush Theory Including Reorganization Energy, *J. Phys. Chem. B*, 2021, **125**, 2696–2706.

24 P. Khammultri, P. Chasing, C. Chitpakdee, S. Namuangruk, T. Sudyoatsuk and V. Promarak, Red to orange thermally activated delayed fluorescence polymers based on 2-(4-(diphenylamino)-phenyl)-9H-thioxanthen-9-one-10,10-dioxide for efficient solution-processed OLEDs, *RSC Adv.*, 2021, **11**, 24794–24806.

25 J. M. Teng, D. W. Zhang, Y. F. Wang and C. F. Chen, Chiral Conjugated Thermally Activated Delayed Fluorescent Polymers for Highly Efficient Circularly Polarized Polymer Light-Emitting Diodes, *ACS Appl. Mater. Interfaces*, 2022, **14**, 1578–1586.

26 S. Liu, Y. Tian, L. Yan, S. Wang, L. Zhao, H. Tian, J. Ding and L. Wang, Color Tuning in Thermally Activated Delayed Fluorescence Polymers with Carbazole and Tetramethylphenylene Backbone, *Macromolecules*, 2023, **56**, 876–882.

27 T. Wang, K. Li, B. Yao, Y. Chen, H. Zhan, Z. Xie, G. Xie, X. Yi and Y. Cheng, Rigidity and Polymerization Amplified Red Thermally Activated Delayed Fluorescence Polymers for Constructing Red and Single-Emissive-Layer White OLEDs, *Adv. Funct. Mater.*, 2020, **30**, 2002493.

28 T. Wang, K. Li, B. Yao, Y. Chen, H. Zhan, G. Xie, Z. Xie and Y. Cheng, Effect of molecular weight on photoluminescence and electroluminescence properties of thermally activated delayed fluorescence conjugated polymers, *Chem. Eng. J.*, 2023, **452**, 139123.

29 Y. Wang, Y. Zhu, G. Xie, H. Zhan, C. Yang and Y. Cheng, Bright white electroluminescence from a single polymer containing thermally activated delayed fluorescence unit and solution-processed orange OLED of approaching 20% external quantum efficiency, *J. Mater. Chem. C*, 2017, **5**, 10715–10720.

30 S. Y. Lee, T. Yasuda, H. Komiyama, J. Lee and C. Adachi, Thermally Activated Delayed Fluorescence Polymers for Efficient Solution-Processed Organic Light-Emitting Diodes, *Adv. Mater.*, 2016, **28**, 4019–4024.

31 Y. Zhu, Y. Zhang, B. Yao, Y. Wang, Z. Zhang, H. Zhan, B. Zhang, Z. Xie, Y. Wang and Y. Cheng, Synthesis and Electroluminescence of a Conjugated Polymer with Thermally Activated Delayed Fluorescence, *Macromolecules*, 2016, **49**, 4373.

32 J. Rao, L. Yang, X. Li, L. Zhao, S. Wang, J. Ding and L. Wang, Meta Junction Promoting Efficient Thermally Activated

Delayed Fluorescence in Donor-Acceptor Conjugated Polymers, *Angew. Chem., Int. Ed.*, 2020, **59**, 17903–17909.

33 P. K. Qiang Wei, Yevhen Karlov, Xianping Qiu, Hartmut Komber, Karin Sahre, Anton Kiriy, Ramunas Lygaitis, Simone Lenk and Sebastian Reineke, Brigitte Voit, Conjugation-Induced Thermally Activated Delayed Fluorescence (TADF): From Conventional Non-TADF Units to TADF-Active Polymers, *Adv. Funct. Mater.*, 2017, **27**, 1605051.

34 Y. Li, Q. Wei, L. Cao, F. Fries, M. Cucchi, Z. Wu, R. Scholz, S. Lenk, B. Voit, Z. Ge and S. Reineke, Organic Light-Emitting Diodes Based on Conjugation-Induced Thermally Activated Delayed Fluorescence Polymers: Interplay Between Intra-and Intermolecular Charge Transfer States, *Front. Chem.*, 2019, **7**, 688.

35 J. Rao, X. Liu, X. Li, L. Yang, L. Zhao, S. Wang, J. Ding and L. Wang, Bridging Small Molecules to Conjugated Polymers: Efficient Thermally Activated Delayed Fluorescence with a Methyl-Substituted Phenylene Linker, *Angew. Chem., Int. Ed.*, 2020, **59**, 1320–1326.

36 H. Zhan, Y. Wang, K. Li, Y. Chen, X. Yi, K. Bai, G. Xie and Y. Cheng, Saturated Red Electroluminescence From Thermally Activated Delayed Fluorescence Conjugated Polymers, *Front. Chem.*, 2020, **8**, 332.

37 Y. Liu, S. Yan and Z. Ren,  $\pi$ -Conjugated polymeric light emitting diodes with sky-blue emission by employing thermally activated delayed fluorescence mechanism, *Chem. Eng. J.*, 2021, **417**, 128089.

38 L. Hua, Y. Liu, H. Zhao, S. Chen, Y. Zhang, S. Yan and Z. Ren, Constructing High-Efficiency Orange-Red Thermally Activated Delayed Fluorescence Polymers by Excited State Energy Levels Regulation via Backbone Engineering, *Adv. Funct. Mater.*, 2023, 2303384.

39 Y. Liu, Y. Wang, C. Li, Z. Ren, D. Ma and S. Yan, Efficient Thermally Activated Delayed Fluorescence Conjugated Polymeric Emitters with Tunable Nature of Excited States Regulated via Carbazole Derivatives for Solution-Processed OLEDs, *Macromolecules*, 2018, **51**, 4615.

40 M. Einzinger, T. Zhu, P. de Silva, C. Belger, T. M. Swager, T. Van Voorhis and M. A. Baldo, Shorter Exciton Lifetimes via an External Heavy-Atom Effect: Alleviating the Effects of Bimolecular Processes in Organic Light-Emitting Diodes, *Adv. Mater.*, 2017, **29**, 1701987.

41 H. Malissa, M. Kavand, D. P. Waters, K. J. van Schooten, P. L. Burn, Z. V. Vardeny, B. Saam, J. M. Lupton and C. Boehme, Room-temperature coupling between electrical current and nuclear spins in OLEDs, *Science*, 2014, **345**, 1487–1490.

42 Y. Liu, G. Xie, Z. Ren and S. Yan, Thermally Activated Delayed Fluorescence Polymer Emitters with Tunable Emission from Yellow to Warm White Regulated by Triphenylamine Derivatives, *ACS Appl. Polym. Mater.*, 2019, **1**, 2204.

43 R. H. Friend, R. W. Gymer, A. B. Holmes, J. H. Burroughes, R. N. Marks, C. Taliani, D. D. C. Bradley, D. A. Dos Santos, J. L. Bre das, M. Lo È Gdlund and W. R. Salaneck, Electroluminescence in conjugated polymers, *Nature*, 1999, **397**, 121–128.

44 Y. Wang, Y. Zhu, X. Lin, Y. Yang, B. Zhang, H. Zhan, Z. Xie and Y. Cheng, Efficient non-doped yellow OLEDs based on thermally activated delayed fluorescence conjugated polymers with acridine/carbazole donor backbone and triphenyltriazine acceptor pendant, *J. Mater. Chem. C*, 2018, **6**, 568–574.

45 Y. Yang, S. Wang, Y. Zhu, Y. Wang, H. Zhan and Y. Cheng, Thermally Activated Delayed Fluorescence Conjugated Polymers with Backbone-Donor/Pendant-Acceptor Architecture for Nondoped OLEDs with High External Quantum Efficiency and Low Roll-Off, *Adv. Funct. Mater.*, 2018, **28**, 1706916.

46 Y. Zhu, Y. Yang, Y. Wang, B. Yao, X. Lin, B. Zhang, H. Zhan, Z. Xie and Y. Cheng, Improving Luminescent Performances of Thermally Activated Delayed Fluorescence Conjugated Polymer by Inhibiting the Intra- and Interchain Quenching, *Adv. Opt. Mater.*, 2018, **6**, 1701320.

47 Y. Yang, K. Li, C. Wang, H. Zhan and Y. Cheng, Effect of a Pendant Acceptor on Thermally Activated Delayed Fluorescence Properties of Conjugated Polymers with Backbone-Donor/Pendant-Acceptor Architecture, *Chem. – Asian J.*, 2019, **14**, 574–581.

48 Y. Yang, Y. Zhu, Y. Wang, S. Wang, H. Zhan and Y. Cheng, Synthesis and electroluminescent performance of thermally activated delayed fluorescence-conjugated polymers with simple formylphenyl as pendant acceptor, *J. Polym. Sci. Pol. Chem.*, 2018, **56**, 1989–1996.

49 Y. Liu, L. Hua, S. Yan and Z. Ren, Halogenated  $\pi$ -conjugated polymeric emitters with thermally activated delayed fluorescence for highly efficient polymer light emitting diodes, *Nano Energy*, 2020, **73**, 104800.

50 Z. Zhao, Y. Liu, L. Hua, S. Yan and Z. Ren, Activating Energy Transfer Tunnels by Tuning Local Electronegativity of Conjugated Polymeric Backbone for High-Efficiency OLEDs with Low Efficiency Roll-Off, *Adv. Funct. Mater.*, 2022, **32**, 2200018.

51 Z. Zhao, X. Tong, Y. Liu, R. Wan, H. Li, S. Yan and Z. Ren, Hyperbranched Conjugated Polymer with Multiple Charge Transfer Enables High-Efficiency Nondoped Red Electroluminescence with Low Driving Voltage, *ACS Appl. Mater. Interfaces*, 2023, **15**, 4257–4266.

52 S. Shao, S. Wang, X. Xu, Y. Yang, J. Lv, J. Ding, L. Wang, X. Jing and F. Wang, Bipolar Poly(arylene phosphine oxide) Hosts with Widely Tunable Triplet Energy Levels for High-Efficiency Blue, Green, and Red Thermally Activated Delayed Fluorescence Polymer Light-Emitting Diodes, *Macromolecules*, 2019, **52**, 3394–4303.

53 M. K. Hung, K. W. Tsai, S. Sharma, J. Y. Wu and S. A. Chen, Acridan-Grafted Poly(biphenyl germanium) with High Triplet Energy, Low Polarizability, and an External Heavy-Atom Effect for Highly Efficient Sky-Blue TADF Electroluminescence, *Angew. Chem., Int. Ed.*, 2019, **58**, 11317–11323.

54 M. K. Hung, S. T. Chung, S. Sharma, K. W. Tsai, J. Y. Wu and S. A. Chen, Poly(acridan-grafted biphenyl germanium) with High Triplet Energy as a Universal Host for High-Efficiency Thermally Activated Delayed Fluorescence Full-Color

Devices and Their Hybrid with Phosphor for White Light Electroluminescence, *ACS Appl. Mater. Interfaces*, 2022, **14**, 55873–55885.

55 Y. Liu, X. Tong, X. Chen, Y. Wang, S. Ying, Z. Ren and S. Yan, Enhanced Upconversion of Triplet Excitons for Conjugated Polymeric Thermally Activated Delayed Fluorescence Emitters by Employing an Intramolecular Sensitization Strategy, *ACS Appl. Mater. Interfaces*, 2021, **13**, 8997–9005.

56 Y. Olivier, J. C. Sancho-Garcia, L. Muccioli, G. D'Avino and D. Beljonne, Computational Design of Thermally Activated Delayed Fluorescence Materials: The Challenges Ahead, *J. Phys. Chem. Lett.*, 2018, **9**, 6149–6163.

57 M. Moral, L. Muccioli, W. J. Son, Y. Olivier and J. C. Sancho-Garcia, Theoretical rationalization of the singlet-triplet gap in OLEDs materials: impact of charge-transfer character, *J. Chem. Theory Comput.*, 2015, **11**, 168–177.

58 H. Sun, C. Zhong and J.-L. Brédas, Reliable Prediction with Tuned Range-Separated Functionals of the Singlet-Triplet Gap in Organic Emitters for Thermally Activated Delayed Fluorescence (TADF), *J. Chem. Theory Comput.*, 2015, **11**, 3851–3858.

59 T. Northey and T. J. Penfold, The intersystem crossing mechanism of an ultrapure blue organoboron emitter, *Org. Electron.*, 2018, **59**, 45–48.